

Oxidative stress and ROS metabolism via down-regulation of sirtuin 3 expression in *Cmah*-null mice affect hearing loss

Deug-Nam Kwon*, Woo-Jin Park*, Yun-Jung Choi, Sangiliyandi Gurunathan, and Jin-Hoi Kim

Department of Animal Biotechnology, Konkuk University, Seoul 143-701, Republic of Korea

* Contributed equally to this work

Key words: hearing loss, CMP-N-acetylneuraminic acid hydroxylase, ROS metabolism, mitochondria dysfunction, oxidative stress

Abbreviations: AHL: age-related hearing loss; Sirt3: sirtuin3; *Cmah*: CMP-N-acetylneuraminic acid hydroxylase; ROS: reactive oxygen species; KEGG: Kyoto Encyclopedia of Genes and Genome; DAVID: Database for Annotation, Visualization and Integrated Discovery; WT: wild-type; Hif1 α : hypoxia-inducible factor 1-alpha; Foxo3a: forkhead box O3a; Foxo1: forkhead box protein O; MnSod: manganese superoxide dismutase 2; RT-qPCR: quantitative real-time polymerase chain reaction; SV: scala vestibule; SM: scala media; ST: scala tympani; SG: spiral ganglion; BM: basilar membrane; RM: reissner's membrane; Sv: stria vascularis; OT: otoconia; OM: otolithic membrane; NHC & SC: neuroepithelial hair cells and supporting cells; HC: hair cells; OHCs: outer hair cells; SL: spiral lamina.

Received: 07/10/15; **Accepted:** 08/23/15; **Published:** 08/29/15

Correspondence to: Jin-Hoi Kim, PhD; **E-mail:** jhkim541@konkuk.ac.kr

Copyright: Kwon et al. This is an open-access article distributed under the terms of the Creative Commons Attribution License, which permits unrestricted use, distribution, and reproduction in any medium, provided the original author and source are credited

Abstract: CMP-Neu5Ac hydroxylase (*Cmah*) disruption caused several abnormalities and diseases including hearing loss in old age. However, underlying molecular mechanisms that give rise to age-related hearing loss (AHL) in *Cmah*-null mouse are still obscure. In this study, *Cmah*-null mice showed age-related decline of hearing associated with loss of sensory hair cells, spiral ganglion neurons, and/or stria vascularis degeneration in the cochlea. To identify differential gene expression profiles and pathway associated with AHL, we performed microarray analysis using Illumina MouseRef-8 v2 Expression BeadChip and pathway-focused PCR array in the cochlear tissues of *Cmah*-null mouse. Pathway and molecular mechanism analysis using differentially expressed genes provided evidences that altered biological pathway due to oxidative damage by low expressed antioxidants and dysregulated reactive oxygen species (ROS) metabolism. Especially, low sirtuin 3 (*Sirt3*) gene expressions in *Cmah*-null mice decreased both of downstream regulator (*Foxo1* and *MnSod*) and regulatory transcription factor (*Hif1 α* and *Foxo3a*) gene expression. Taken together, we suggest that down-regulation of *Sirt3* expression leads to oxidative stress and mitochondrial dysfunction by regulation of ROS and that it could alter various signaling pathways in *Cmah*-null mice with AHL.

INTRODUCTION

N-glycolylneuraminic acid (Neu5Gc) is generated by hydroxylation of CMP-Neu5Ac to CMP-Neu5Gc, catalyzed by CMP-Neu5Ac hydroxylase (*Cmah*) [1, 2]. However, humans lack this common mammalian cell surface molecule, Neu5Gc, due to inactivation of the *Cmah* gene during evolution [3, 4]. Previous studies showed that disruption of *Cmah* gene affect various biological processes of animals [5, 6]. Our recent study has suggested that *Cmah*-null mice could be a useful model for studying diabetes with dysregulation of insulin/

PI3K-AKT signaling [7]. In another study, *Cmah*-null mouse showed histological abnormalities of the inner ear occurred in older mice, which had impaired hearing [5]. On the other hand, it was reported in a study that, in a senescence-accelerated mouse, prone 8 (SAMP8) strain mouse shows premature hearing loss and cochlear degeneration repeating the processes noticed in human presbycusis (*i.e.*, stria, sensory, and neural degeneration) [8]. The molecular mechanisms correlated with premature age-related hearing loss (AHL) in SAMP8 mice comprises oxidative stress, distorted levels of antioxidant enzymes, and decreased

activity of some complexes which as a result leads to chronic inflammation and prompting of apoptotic cell death pathways [8]. In another studies, rat F344/NHsd strain showed an increased mitochondrial DNA deletions in the cochlea at 6- and 9-months of age [9, 10]. As a result, mitochondrial DNA deletions or mutations causes impairment in mitochondrial function and eventually leads to buildup of cochlear oxidative stress and consequent cochlear degeneration and AHL [11]. Even though there is growing recognition that oxidative stress and reactive oxygen species (ROS) may be an important factor for underlying mechanism of hearing loss, the studies of molecular mechanisms of AHL is still infancy in *Cmah*-null mouse.

Recent study provided a possible mechanism of sirtuin 3 (Sirt3) in ROS and oxidative stress induced metabolism in mammals [12, 13]. Sirtuins are NAD⁺-dependent protein deacetylases [14]. They possess the ability to regulate life span in lower organisms and have turned up as immense cellular fate regulators and mammalian biology [15]. There are seven sirtuins in mammals; they demonstrate diverse cellular localization [16, 17]. Among them, Sirt3 localized in mitochondria stimulation results in activation of oxidative metabolism through deacetylation of numerous mitochondrial enzymes [18, 19]. Sirt3 has been found to predominantly regulate the production of ROS at the electron transport chain (ETC), further the detoxification of ROS via activation of antioxidant enzymes [20-25]. A current study implied that mitochondrial Sirt3 arbitrates the anti-aging effects of calorie restriction (CR) on AHL by promoting the glutathione-mediated mitochondrial antioxidant defense system in mice [23]. As CR is recognized to provoke Sirt3 protein levels in wild-type (WT) mice, there is a possibility that Sirt3 expression levels can mediate ROS management, mitochondrial integrity, and sensory function, at least in those neurons that constrain hearing [26-28]. CR-mediated aging retardation regulated by Sirt3 in mammal. However, CR failed and impaired to reduce oxidative damage in multiple tissues of *Sirt3* null mouse compare to control and it leads to the progression of AHL [29].

Despite growing interest in the relationship between loss of *Cmah* activity and age-related hearing loss, how genome-wide altered gene expression in the cochlear tissues of *Cmah*-null mouse affects hearing loss with aging remains unclear. In this study, we first explored differential gene expression profile in the cochlear tissues of *Cmah*-null mouse. We performed the functional enrichment analyses using annotations from both Gene Ontology (GO) and pathways. More importantly, we identified the pathway that related to

the oxidative damage and ROS metabolism, supporting the pathogenesis hypothesis of age-related dysfunction. Finally, we analyzed the expression of their genes that involved Sirtuins, oxidative stress regulation, Wnt signaling, mitochondrial dysfunction identified by KEGG (Kyoto Encyclopedia of Genes and Genome) pathway analysis on microarray and a pathway-focused PCR array to address the mechanisms underlying AHL in *Cmah*-null mouse. In conclusion, we suggest a hypothetical model that down-regulated Sirt3 lead to oxidative damage and mitochondrial dysfunction by ROS and could alter various signaling pathways in *Cmah*-null mice with AHL. In this study, we propose a possible hypothetical model that down-regulated *Sirt3* lead to oxidative damage and mitochondrial dysfunction by ROS and it could alter various signaling pathways involved in *Cmah*-null mice with AHL.

RESULTS

***Cmah* disruption result in histological abnormalities in vestibular otoconial epithelia and the cochlear sensory epithelium, and neuronal cell loss of inner ears**

Cmah-null mouse, like the previous observations, showed age-related hearing loss [5, 30]. To determine the lack of *CMAH* protein expression, we performed immunohistochemistry (IHC) in inner ear from WT- and *Cmah*-null mice. As shown in Fig. 1A, the Neu5Gc, which is a final product by hydroxylation of CMP-Neu5Ac to CMP-Neu5Gc by CMP-Neu5Ac hydroxylase, was highly expressed in the WT, whereas the *Cmah*-null mice were completely deficient in inner ears. In histological analysis, 12 month- but not 5 week-old (Supplementary Fig. 1). *Cmah*-null mice had histological abnormalities in the vestibular otoconial epithelia and the cochlear sensory epithelium of inner ears (Fig. 1B). The apical surface of the vestibular otoconial epithelia contains unusual deposits of apparently a cellular material among the stereociliary bundles (Fig. 1B upper). Further, we observed degeneration of outer hair cell throughout the cochlea, with collapse of the outer organ of corti in the basal (high-frequency) turn of 12 month-old mice (Fig. 1B; bottom), whereas both of the cochlear and vestibular sensory epithelia of WT-mice appeared normal, even in older mice. Next, we performed the TUNEL assay to investigate the apoptotic cell death. The result shows significantly increased numbers of apoptotic cells in supporting cells of cochlear tissues from *Cmah*-null mice, compared to control (Fig. 1C).

In order to examine neuronal cell loss in *Cmah*-null mouse, we investigate the several neuronal cell-specific

gene expressions in cochlear tissues. In this study, we examined glial fibrillary acidic protein (GFAP) expression for a neural injury marker or astrocyte marker, neurofilament (NF) expression for an axonal injury marker, vimentin (VIM) expression for a neural precursor cells marker, and enolase (NSE) expression for neuronal specific marker. In IHC, cochlear tissues of *Cmah*-null mice showed significant reductions in expres-

sions of several neuronal cell markers such as GFAP, NSE, NF, and VIM in with respect to control mice (Fig. 1D). Reverse transcriptase quantitative real-time polymerase chain reaction (RT-qPCR) analysis also showed significantly down-regulated gene expression for same neuronal cell markers (*Gfap*, *Nse*, *Nf*, and *Vim*) compared to control (Fig. 1E), indicate that RT-qPCR results mimic IHC results.

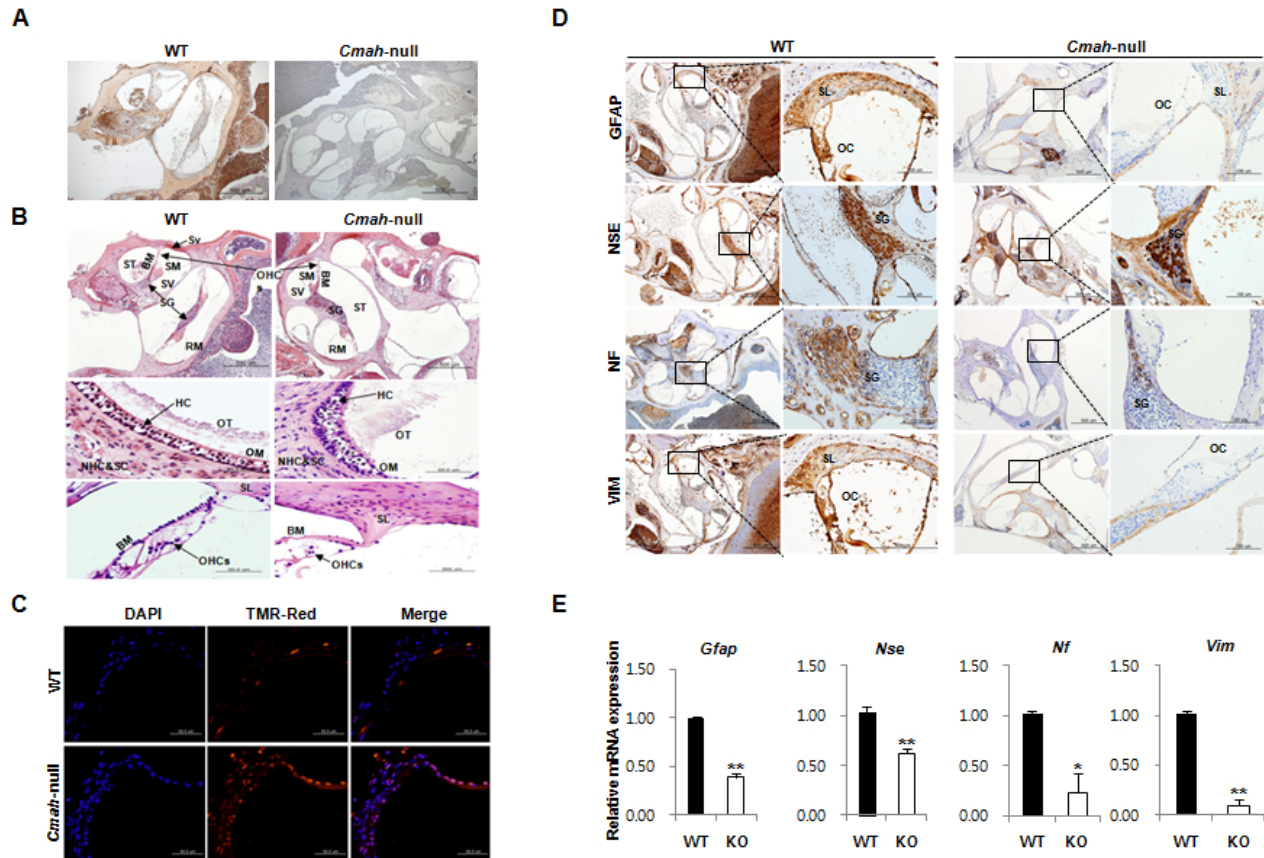


Figure 1. Age-related inner ear abnormality and neuron cell loss in *Cmah*-null mice. (A) Analysis of Neu5Gc expression in cochlear tissues of WT- and *Cmah*-null mice by IHC using a chicken anti-Neu5Gc antibody. (B) Histological abnormality in inner ears of *Cmah*-null mice. Deposition of unusual and apparently a cellular material in the vestibular otoconial epithelia (upper). The area of the outer hair cells showed degeneration of the sensory cells throughout the cochlea in the cochlear sensory epithelium, (bottom). SV: scala vestibule, SM: scala media, ST: scala tympani, SG: spiral ganglion, BM: sasilar membrane, RM: reissner's membrane, Sv: stria vascularis, OT: otoconia, OM: otolithic membrane, NHC & SC: neuroepithelial hair cells and supporting cells, HC: hair cells, OHCs: outer hair cells, SL: Spiral lamina. (C) Apoptotic cell death in the cochlea of *Cmah*-null mice. TUNEL labeling performed on paraffin sections the cochlea from WT- and *Cmah*-null mice. (D) The expression of ganglion cells in cochlear tissues from WT- and *Cmah*-null mice by IHC. Rectangular box indicate a higher magnification images (5x) in left panel. GFAP: Glial fibrillary acidic protein, NSE: Neuron specific enolase, NF: Neurofilament, VIM: Vimentin. SL: spiral lamina, OC: organ of corti, SG: spiral ganglion. (E) mRNA expression pattern of neuronal cell markers in cochlear tissues from WT- and *Cmah*-null mice. RT-qPCR was used to measure the expression of *Gfap*, *Nse*, *Nf*, and *Vim* in the cochlea from WT- and *Cmah*-null mice.

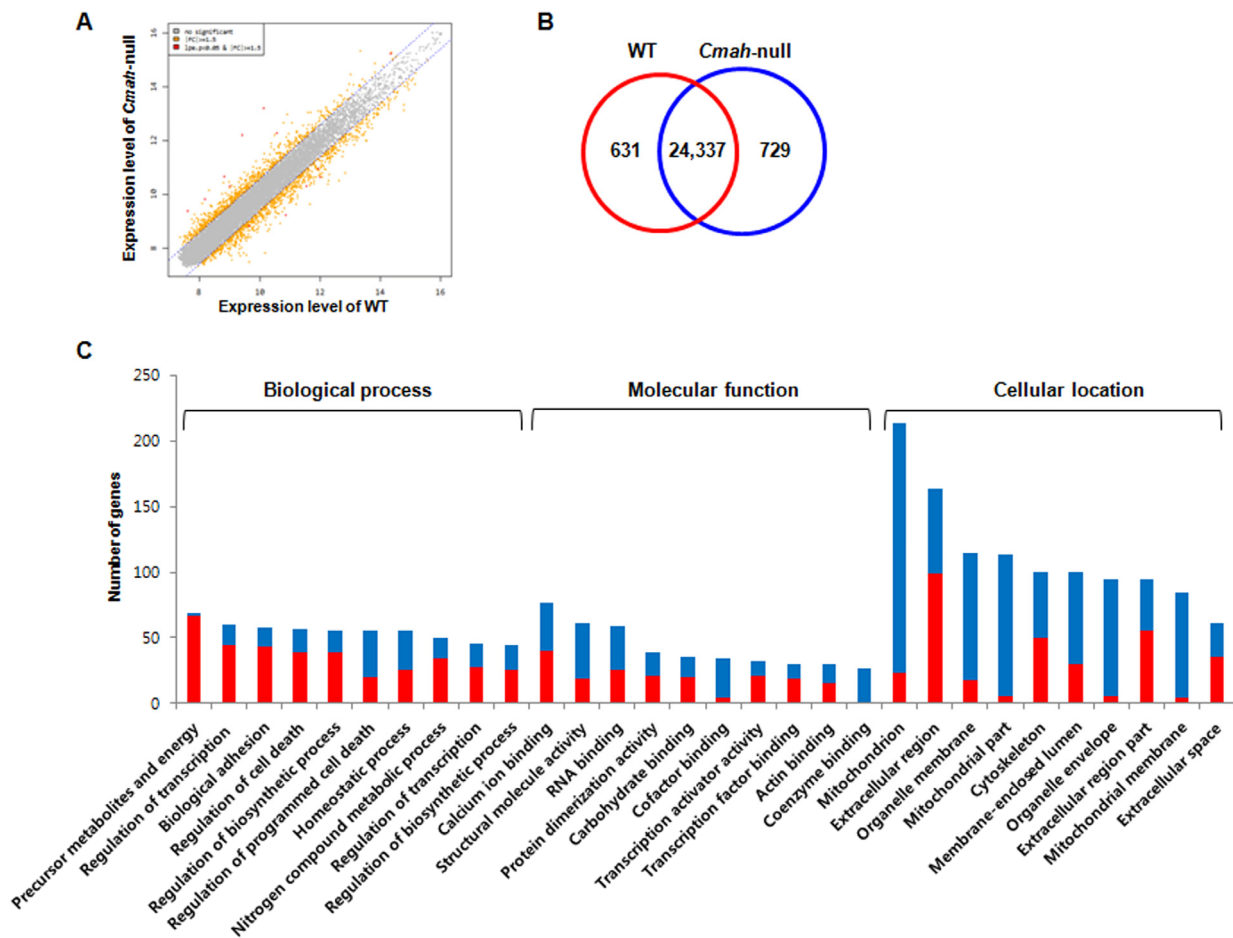


Figure 2. Gene expression profile in cochlea of *Cmah*-null mice. (A) Scatterplot of normalized mRNA expression by microarray. Data are log₂ normalized. Grey- and orange-spots indicate no significant genes and up- or down-regulated genes, with more than 1.5-fold change. (B) Venn diagram showing differential expression of genes in the cochlear tissues of *Cmah*-null mice. Numbers in red and blue Venn diagram present up- and down- regulated genes, respectively. (C) The differentially up- or down-regulated genes were clarified according to biological process, molecular function, and cellular component. GO classification significantly enriched with a Benjamini-Hochberg corrected P value < 0.05 among all differentially expressed genes with ≥ 1.5 -fold expression between WT- and *Cmah*-null mice.

Differential gene expression profile in cochlea of *Cmah*-null mice

Expression profiles in cochlear tissues of WT- and *Cmah*-null mice (n=3, respectively) were compared using an Illumina MouseRef-8 v2 Expression BeadChip, which is composed of 25,697 probe sets for mouse mRNA. To analyze differential gene expression in WT- and *Cmah*-null mice, we focused on the gene expressions, which showed ≥ 1.5 folds changes with a significant p-value ($p < 0.05$). In this study, we performed scatter plot analysis in order to estimate global gene expression change. As shown in Fig. 2A, mRNA expression was normalized by the scatter plots:

of 25,697 genes, 631 genes were up-regulated, whereas 729 genes were down-regulated in *Cmah*-null mice-derived cochlear tissues compared to control mice-derived cochlear tissues (Fig. 2B). Additional File 1 and 2 showed complete lists of these genes.

Functional analysis of differentially expressed genes in cochlea of *Cmah*-null mice

To explore their biological functions, GO classification by functional annotation of the DAVID (Database for Annotation, Visualization and Integrated Discovery) tools categorize each genes with significant differential expression in cochlea of *Cmah*-null mice. Fig. 2C

showed the top 10 enriched functional annotations in three categories according to GO classification. These functional annotations consisted of generation of pre-

cursor metabolites and energy (69 genes), regulation of transcription from RNA polymerase II promoter (60 genes), biological adhesion (58 genes), regulation of cell

Table 1. KEGG pathway analysis in the cochlear tissues of *Cmah*-null mice

Term	Count	P value	Genes
Oxidative phosphorylation	47	3.47E-19	<i>Uqcrc2, Ndufb3, Atp5e, Ndufb4, Ndufb5, Ndufb8, Ndufb9, Cyc1, Cox7b, LOC100048613, Atp6v1g2, Atp12a, Ndufb2, Ndufs6, Ndufs4, Ndufs8, Cox6b1, Cox6b2, Ndufs3, Cox17, Ndufs2, Atp5h, Ndufa4, Ndufa5, Ndufa2, Atp5j2, Ndufa3, Cox7a2, Ndufa8, Cox8b, Cox7a1, Ndufa9, Ndufa6, Ndufa7, Ndufc2, Atp5f1, Ndufc1, Ndufa1, Cox6c, Sdhd, Atp6v1a, Uqcrh, Ndufv2, Sdhd, Atp5c1, Atp6v0a1, Atp5a1</i>
Huntington's disease	54	1.54E-17	<i>Uqcrc2, Atp5e, Pparg, Cyc1, LOC100048613, LOC100046796, Ndufs6, Bdnf, Ndufs4, Ndufs8, Ndufs3, Atp5h, Ndufs2, Cysc, Ndufc2, Ndufc1, Ppargc1a, Dctm1, Cox6c, Uqcrh, Atp5c1, Ndufb3, Ndufb4, Polr2g, Ndufb5, Ndufb8, Ndufb9, Cox7b, Ndufb2, Dnal1, Cox6b1, Cox6b2, Hap1, Ndufa4, Trp53, Ndufa5, Ndufa2, Cox7a2, Ndufa3, Cox7a1, Cox8b, Ndufa8, Ndufa9, Ndufa6, Creb1, Ndufa7, Atp5f1, Ucp1, Ndufa1, Sod2, Sdhd, Ndufv2, Sdhd, Atp5a1</i>
Parkinson's disease	42	9.64E-15	<i>Uqcrc2, Ndufb3, Atp5e, Ndufb4, Ndufb5, Ndufb8, Ndufb9, Cyc1, Cox7b, LOC100048613, Ndufb2, Ndufs6, Ndufs4, Ndufs8, Cox6b1, Cox6b2, Ndufs3, Ndufs2, Atp5h, Ndufa4, Ndufa5, Ndufa2, Ndufa3, Cox7a2, Ndufa8, Cox8b, Cox7a1, Ndufa9, Ndufa6, Ndufa7, Cysc, Ndufc2, Atp5f1, Ndufc1, Ndufa1, Cox6c, Sdhd, Uqcrh, Ndufv2, Sshd, Atp5c1, Atp5a1</i>
Alzheimer's disease	48	1.72E-13	<i>Ndufb3, Uqcrc2, Atp5e, Ndufb4, Ndufb5, Ndufb8, Ndufb9, Cyc1, Cox7b, LOC100048613, Ndufb2, Ndufs6, Ndufs4, Ndufs8, Cox6b1, Il1b, Cox6b2, Ndufs3, Ndufs2, Atp5h, Ndufa4, Ndufa5, Ndufa2, Ndufa3, Cox7a2, Ndufa8, Cox8b, Cox7a1, Ndufa9, Ndufa6, Ndufa7, LOC100048622, Cysc, Ndufc2, Atp5f1, Ndufc1, Ndufa1, Cox6c, Ncstn, Sdhd, Uqcrh, Atp2a3, Ndufv2, Sdhd, Calm4, Atp5c1, Atp5a1, Calm2</i>
Fatty acid metabolism	17	1.80E-07	<i>Cpt1b, Acaa2, Acadsb, Acadm, Cpt2, Acads, Adh5, Echs1, Acat2, Acadl, Peci, Dci, Hadhb, Acadvl, Acs11, Adh1, Acs15</i>
Citrate cycle (TCA cycle)	13	2.25E-06	<i>Sdhd, Idh3g, Aco2, Suclg1, Dld, Sdhd, Idh2, Idh1, Pdha1, Fhl, Pdhd, Pck1, Mdh1</i>
Cardiac muscle contraction	15	0.003403691	<i>Uqcrc2, Cacna2d1, Actc1, Cox7a2, Cox8b, Cox7a1, Atp1b2, LOC100048613, Cox7b, Cyc1, Cacng5, Cox6c, Uqcrh, Cox6b1, Cox6b2</i>
Glycolysis / Gluconeogenesis	13	0.007452722	<i>Pfkfb, Adh5, Pfkfb, Fbp2, Pdhd, Aldh3a1, Pck1, Pgm2, Tpi1, Adh1, Dld, Eno3, Pdha1</i>
Glutathione metabolism	10	0.021733591	<i>Mgst3, Gstm1, Gpx4, Gpx3, Idh2, Gstz1, Idh1, Anpep, Gclm, Mgst1</i>
Proteasome	9	0.032475591	<i>Psmb5, Psmb7, Psm14, Psm6, Psm4, Psm3, Shfm1, Psme4, Psm6</i>
Wnt signaling pathway	12	0.046687622	<i>Trp53, Wnt10a, Fzd10, Ccnd1, Wnt7b, Wnt4, Btrc, LOC100048622, Wnt6, Axin2, Prkx, Nfatc1</i>

Number of the observed differentially expressed genes in the category. P values is less than 0.05 (P<0.05).

death (57 genes), regulation of biosynthetic process (55 genes), regulation of programmed cell death (55 genes), homeostatic process (55 genes), regulation of nitrogen compound metabolic process (50 genes), regulation of transcription (46 genes), regulation of biosynthetic process (44 genes) for biological process; calcium ion binding (77 genes), structural molecule activity (61 genes), RNA binding (59 genes), protein dimerization activity (39 genes), carbohydrate binding (35 genes), cofactor binding (34 genes), transcription activator activity (32 genes), transcription factor binding (30 genes), actin binding (30 genes), coenzyme binding (27 genes) for molecular function; mitochondrion (213 genes), extracellular region (163 genes), organelle membrane (115 genes), mitochondrial part (113 genes), cytoskeleton (100 genes), membrane-enclosed lumen (100 genes), organelle envelope (95 genes), extracellular region part (94 genes), mitochondrial membrane (84 genes), and extracellular space (61 genes) for cellular component.

Next, we examined differentially expressed genes that are enriched in pathways by KEGG pathway analysis. Table 1 show the 11 most significantly enriched pathways. Of note, most of them are closely associated with oxidative damage and metabolism, supporting the pathogenesis hypothesis of age-related dysfunction. These results are consistent with prior knowledge of AHL [5, 11, 29]. In addition, ingenuity analysis identifi-

ed more putative diseases and disorders in cochlear tissues of *Cmah*-null mice. These are as follows: neurological disease, psychological disorders, skeletal and muscular disorders, infectious disease, and hereditary disorder (Table 2). Among them, neurological disease consisted of movement disorders (237 genes, 1.65E-13), disorder of basal ganglia (178 genes, 7.88E-13), neuromuscular disease (190 genes, 5.69E-11), neurological signs (151 genes, 6.19E-10), dyskinesia (143 genes, 1.34E-09), Huntington's disease (135 genes, 1.44E-09), progressive motor neuropathy (97 genes, 7.78E-06), damage of brain (31 genes, 1.25E-04), seizures (77 genes, 2.22E-04), hypomyelination (11 genes, 4.76E-04), damage of cerebral cortex (11 genes, 8.94E-04), dysmyelination of sciatic nerve (4 genes, 9.96E-04), and seizure disorder (84 genes, 1.09E-03) (Fig. 3A). Furthermore, we determined the canonical pathways by IPA tool using genes differentially expressed in cochlear tissues of *Cmah*-null mice. Of them, the pathway classified aging-related functional groups as follow: glutathion-mediated detoxification, protein ubiquitination pathway, phagosome maturation, mitochondrial dysfunction, glutathione redox reaction I, acetyl-coA biosynthesis, oxidative phosphorylation, and TCA cycle for oxidative stress and mitochondrial dysfunction (Group I) and Wnt/ β -catenin signaling (Group II) (Fig. 3B). Taken together, these results provide further information for evaluation of the potential effects and altered functions caused by *Cmah* gene disruption.

Table 2. Disease and disorders identified by Ingenuity Pathway Analysis in the cochlear tissues of *Cmah*-null mice

Diseases and Disorders		
Name	P value	#Molecules
Neurological Disease	9.49E-14~1.75E-03	385
Psychological Disorders	5.14E-13~1.30E-09	178
Skeletal and Muscular Disorders	2.99E-10~1.60E-03	472
Infectious Disease	4.20E-10~1.58E-03	298
Hereditary Disorder	1.30E-09~1.60E-03	163

P values represent significance of overrepresentation of candidate genes within respective gene groups. P value ranges indicate values for various disease subclassifications (not shown).

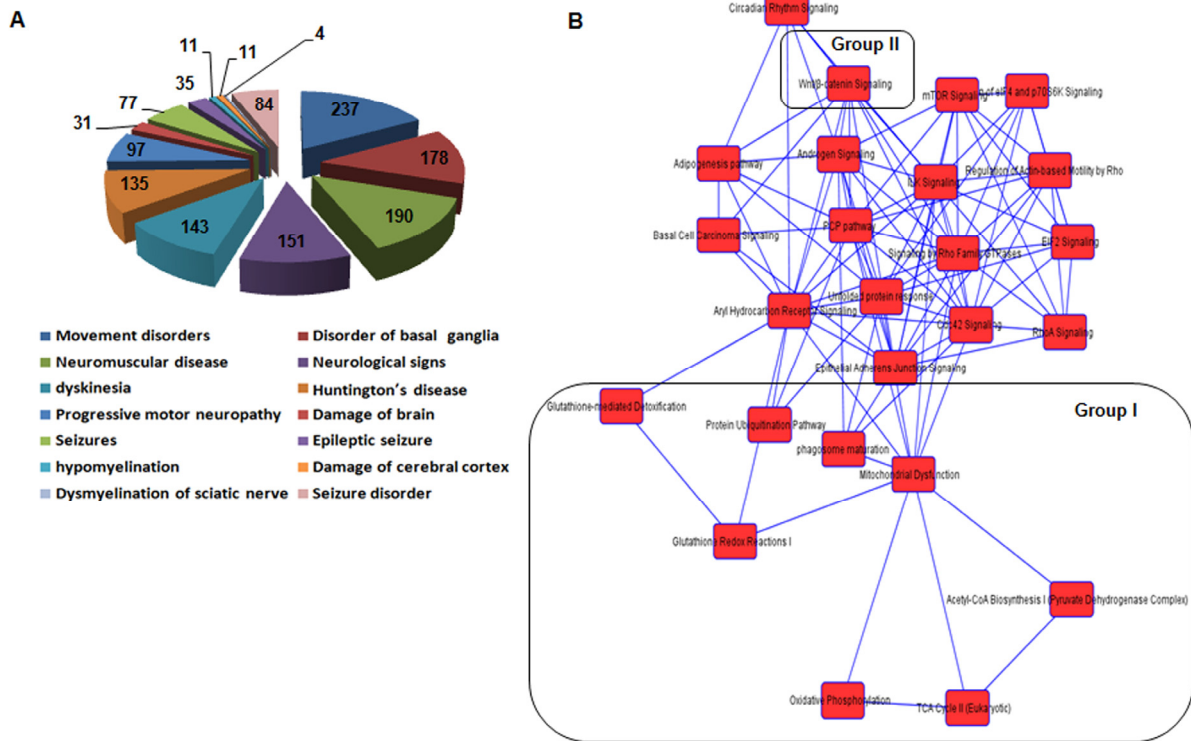


Figure 3. Functional categorization of neurological disease and network of canonical pathways objected by IPA using genes differentially expressed in the cochlea of *Cmah*-null mice. (A) Pie chart analysis of the disease or functions annotation for neurological disease. (B) The network of canonical pathways highlights the relationships between pathways and classifies the functional groups by IPA analysis. Group I and II represent oxidative stress and mitochondrial dysfunction-related signaling (Group I), and Wnt/ β -catenin signaling (Group II), respectively.

Alteration of genes involved in oxidative damage and ROS metabolism

To clarify differential mRNAs expression of oxidative stress and antioxidant defense-related genes, we examined the expression of genes related to oxidative damage and ROS metabolism pathway in the cochlear tissues from WT- and *Cmah*-null mice, using a pathway-focused PCR array. RT-qPCR analysis revealed a significant down-regulation in most of gene expressions in *Cmah*-null mice with AHL, except one gene, *ApoE* (Table 3). Down-regulated genes consisted of 3 specific subsets for oxidative damage and dysregulated ROS metabolism as follows: 1) glutathion peroxidases (*Gpxs*), peroxiredoxins (*Tpxs*), peroxidases, and antioxidant-related genes, 2) superoxide dismutases (*Sod*), genes involved in superoxide metabolism, genes involved in ROS metabolism, and oxidative damage responsive genes for ROS metabolism, and 3) oxygen transporters. Therefore, these results suggested specific

subsets of oxidative stress genes that appear to play an important role in AHL in the *Cmah*-null mice.

Molecular mechanisms of sirtuins and oxidative stress regulation, and Wnt signaling that involved in *Cmah*-null mice with hearing loss

To address the underlying mechanisms of AHL in *Cmah*-null mouse, we analyzed the expression of their genes that involved sirtuins, oxidative stress regulation, Wnt signaling, mitochondrial dysfunction identified by pathway analysis on microarray and a pathway-focused PCR array. As shown in Fig. 4A, *Sirt3* protein expression was significantly reduced in cochlear tissues of *Cmah*-null mouse, compared to their control. Also, RT-qPCR analysis showed that *Sirt3*, 4, and 5 gene expressions is significantly reduced in *Cmah*-null mice than in controls (Fig. 4B). To determine the expression of AHL related genes in the cochlear tissues of *Cmah*-null mouse, we checked the expression profiles of these

genes on the microarray analysis (Fig. 4C). The result shows that the data sets obtained from the microarray analysis accurately matched with RT-qPCR analysis in *Cmah*-null mouse (Fig. 4C and D). Like that, expressions of *Hif1 α* and *Foxo3a* mRNAs as transcription factor regulated by *Sirt3* as well as *Foxo1* and *MnSod* mRNAs expressions as downstream regulator of *Sirt3* was decreased in *Cmah*-null mice (Fig. 4D).

To observe the regulatory factors in Wnt signaling, which might control by ROS in *Cmah*-null mouse, we analyzed the expression of Wnt signaling-related genes (*Lrp5*, *Lrp6*, *Wnt3a*, *Wnt5a*, *Gsk3 β* , and *Catenin*). The result shows that Wnt signaling-related gene expressions in *Cmah*-null mouse were significantly decreased, whereas the Wnt receptor gene expression was not altered (Fig. 4D). Next, we examined mitochond-

rial dysfunction-related gene expression. The expression of these genes (*Crb1*, *Mtfp1*, *RhoT2*, *Soc2*, and *Atp5f1*) with a role as regulators and mediators of mitochondrial molecular transport was significantly down-regulated (Fig. 4D). We therefore investigated whether altered genes affect the mitochondria expression in sensory neurons of *Cmah*-null mouse by immunofluorescence. As shown in Fig. 4E, mitochondrial positive signals were significantly decreased in *Cmah*-null mice, compared to control mice. Taken together, we proposed a key underlying mechanism for explaining AHL in *Cmah*-null mice (Fig. 4F), suggested that AHL in *Cmah*-null mice was caused by down-regulation of *Sirt3* mRNA expression, which resulted in histological abnormalities in vestibular otoconial epithelia and the cochlear sensory epithelium, and neuronal cell loss in inner ears due to mitochondrial dysfunction by excessive oxidative stress.

Table 3. Alteration of genes involved in oxidative damage and ROS metabolism in the cochlea of *Cmah*-null mice

Subsets	Groups	Genes
Antioxidants	Glutathion Peroxidases (<i>Gpxs</i>)	<i>Gpx1</i> (-45.63), <i>Gpx2</i> (-4.04), <i>Gpx7</i> (-5.55)
	Peroxiredoxins (<i>Tpxs</i>)	<i>Prdx1</i> (-24.50), <i>Prdx4</i> (-107.49)
	Peroxidases	<i>Cat</i> (-5.59), <i>Duox1</i> (-22.85), <i>Epx</i> (-43.83), <i>Lpo</i> (-158.02), <i>Mpo</i> (-5.61), <i>Ptgs2</i> (-68.74), <i>Rag2</i> (-101.27), <i>Serp1b1b</i> (-88.65), <i>Tpo</i> (-1114.36)
	Antioxidants	<i>Alb</i> (-3650.81), <i>Sod1</i> (-31.69), <i>Srxn1</i> (-4.20), <i>Txnrd2</i> (-37.61), <i>Txnrd3</i> (-37.40)
ROS metabolism	Superoxide Dismutases (<i>Sod</i>)	<i>Sod1</i> (-31.69), <i>Sod2</i> (-53.56)
	Genes involved in superoxide metabolism	<i>Cygb</i> (-4.12), <i>Ncf1</i> (-15.17), <i>Ncf2</i> (-26.17), <i>Nos2</i> (-216.32), <i>Nox1</i> (-685.97), <i>Nox4</i> (-59.26), <i>Nox1</i> (-3891.20), <i>Recq14</i> (-42.05), <i>Scd1</i> (-8.50)
	Genes involved in ROS metabolism	<i>Fmo2</i> (-5.95)
	Oxidative Damage Responsive Genes	<i>Als2</i> (-10.64), <i>ApoE</i> (12.54), <i>Cat</i> (-5.59), <i>Ccl5</i> (-51.16), <i>Duox1</i> (-22.85), <i>Epx</i> (-43.83), <i>Ercc2</i> (-9.90), <i>Ercc6</i> (-9.77), <i>Duox1</i> (-55.87), <i>GclC</i> (-18.80), <i>Gpx1</i> (-45.63), <i>Gpx2</i> (-4.04), <i>Gpx7</i> (-5.55), <i>Hmox1</i> (-19.82), <i>Hspa1a</i> (-22.78), <i>Krt1</i> (-5.23), <i>Mpo</i> (-5.61), <i>Nqo1</i> (-7.81), <i>Prdx1</i> (-24.50), <i>Psm5</i> (-7.16), <i>Sod1</i> (-31.69), <i>Tpo</i> (-1114.36), <i>Txn1</i> (-99.46), <i>Txnrd2</i> (-37.61), <i>Ucp3</i> (-41.41), <i>Xpa</i> (-19.89)
Oxygen Transporters		<i>Atr</i> (-9.36), <i>Cygb</i> (-4.12), <i>Dnm2</i> (-6.47), <i>Fancc</i> (-10.66), <i>Ift172</i> (-4.69), <i>Mb</i> (-14.77), <i>Ngb</i> (-257.96)

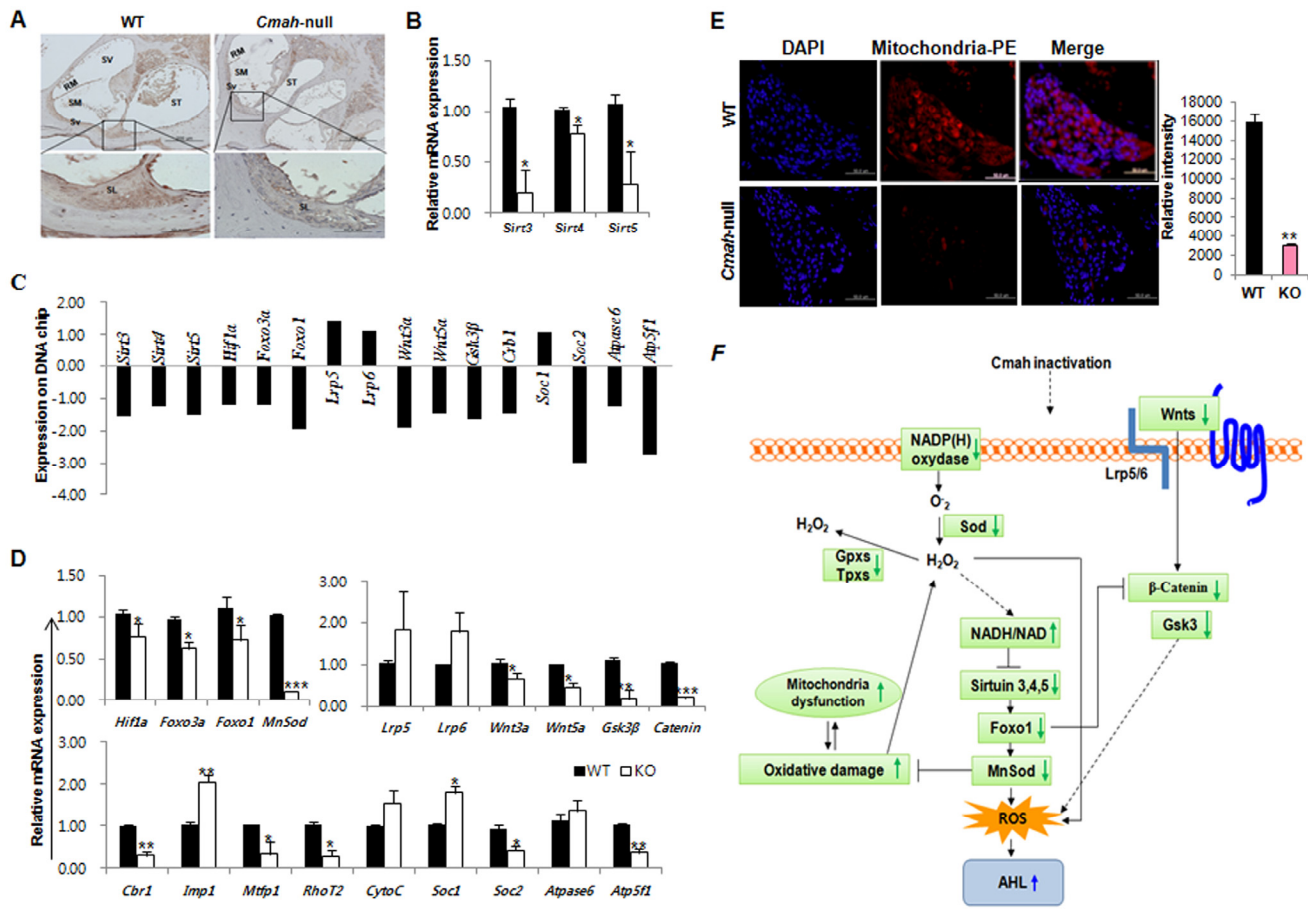


Figure 4. Molecular mechanisms of sirtuins, oxidative stress regulation, and Wnt signaling involved in *Cmah*-null mice. (A) IHC in cochlea of WT- and *Cmah*-null mouse for detection of Sirt3. Bar: 200 um. SV: scala vestibule, RM: reissner's membrane, SM: scala media, ST: scala tympani, Sv: stria vascularis, SL: spiral lamina. (B) Expression levels of sirtuins were determined by RT-qPCR of RNA samples from cochlear tissues of WT- and *Cmah*-null mice. (C) Expression of AHL related genes on the microarray data from cochlear tissues of *Cmah*-null mice. (D) Expression levels of genes involved in the regulatory factor of sirtuin, Wnt signaling, and mitochondrial functional regulation were determined by RT-qPCR of RNA samples from cochlear tissues of WT- and *Cmah*-null mice. (E) Measurement of mitochondrial activity in the cochlea of WT- and *Cmah*-null mice. Immunofluorescence was performed using a mitochondrial marker antibody. The intensity of the fluorescent signal indicates mitochondria numbers or the level of integrity. (F) Summary model describing the molecular mechanisms for sirtuins and oxidative stress regulation, Wnt signaling, and mitochondrial dysfunction by identified RT-qPCR results and array data set. The down-regulated Sirt3 lead to oxidative damage and mitochondrial dysfunction and could be alter various signaling pathways in *Cmah*-null mice with AHL. *Sirt3-5*: NAD-dependent protein deacetylase sirtuin3-5, *Hif1a*: Hypoxia-inducible factor 1-alpha, *Foxo3a*: Forkhead box O3, *Foxo1*: Forkhead box protein O1, *MnSod*: superoxide dismutase 2, mitochondrial, *Lrp5-6*: Low-density lipoprotein receptor-related protein 5-6, *Wnt*: *Wingless*, the *Drosophila melanogaster* segment-polarity gene, and *Integrase-1* the vertebrate homologue, *Gsk3b*: Glycogen synthase kinase 3 beta, *Cbr1*: carbonyl reductase 1, *Imp1*: inner mitochondrial membrane peptidase-like, *Mtfn1*: mitochondrial fission process 1, *RhoT2*: Mitochondrial Rho GTPase 2, *CytoC*: Cytochrome C, *Soc1-2*: soluble oxidase component 1-2.

DISCUSSION

In this study, *Cmah*-null mice showed AHL. To identify a change by hearing loss with aging in *Cmah*-null mice, we have analyzed global gene expression profiling, gene interaction network, and signaling pathway using Illumina Beadchip microarray in inner ear of WT- and

Cmah-null mice. *Cmah*-null mice with hearing loss are closely associated with neurological disease (Alzheimer's disease, Parkinson's disease and Huntington's disease), psychological disorders, skeletal and muscular disorders, infectious disease, and hereditary disorder. These observations are consistent with previous knowledge of AHL, which shows

Alzheimer's disease, Parkinson's disease, and Huntington's disease [31]. Also, we have identified stress response and Wnt signaling abnormality, and mitochondrial dysfunction, which are up- and down-regulated by the loss of *Cmah* activity. Especially, we identified a molecular mechanism of oxidative stress regulated by *Sirt3* expression, which lead to mitochondrial dysfunction by ROS, in *Cmah*-null mice. Therefore, we concluded that *Sirt3* dysfunction in *Cmah*-null mice altered various signaling pathways, which are responsible for the most common sensory disorder in the elderly.

Generally, AHL is closely associated with an impaired inner ear, which generally shows loss of sensory hair cells and/or stria vascularis degeneration in the cochlea and neuronal loss (spiral ganglion neurons) in brain [32]. It is generally well-known that GFAP is a neural injury marker or astrocyte marker; NF for an axonal injury marker, VIM for a neural precursor cells marker in CNS, and NSE for neuronal marker. To this end, we studied the alteration of GFAP, NSE, NF, and VIM in cochlear tissues during different stages of AHL used *Cmah*-null mice mimicking AHL. Immunohistochemically there is combined loss of staining for GFAP, NF, and VIM in cochlear tissues of *Cmah*-null mice, whereas NSE staining patterns was optically not changed (Fig. 1). However, all of *Gfap*, *Nse*, *Nf*, and *Vim* mRNA expressions in *Cmah*-null mice are significantly down-regulated, compared to control. Of note, cochlear tissues of *Cmah*-null mice showed extensive apoptosis, whereas control mouse showed a moderate apoptosis. Our results suggested that there was a potential astrocyte regenerative response to neuron degeneration in the adult cochlear tissues during the onset and progression stages of AHL-like disease. Therefore, the regenerative responses in the adult cochlear tissues of AHL-like mice may be a potential pathway in attempting to repair the degenerated neurons and restore the dysfunctional neural circuitry.

Having identified differentially expressed genes between *Cmah*-null and control mice, we searched for differential gene expression profiles contributing to hearing loss with aging. In this study, we determined the 11 most significantly enriched pathways with differentially expressed genes identified on microarray analysis by KEGG pathway analysis to explore their functional role. Remarkably, most of them are associated with the oxidative stress, metabolism and degenerative nerve diseases, supporting the pathogenesis hypothesis of age-related dysfunction (Table 1). Previous studies suggest that in case of AHL, oxidative stress is playing significant role. ROS

generated in cochleae increase high-intensity noise [33]. Mice lacking antioxidant enzymes demonstrate enhanced age-related cochlear hair cell loss and susceptibility to noise-induced hearing loss [34, 35]. Moreover, oxidative stress increases protein damage, which directly related to age in the cochleae of CBA mice [36]. To address the possibility that in *Cmah*-null mice the cochlear tissues generates excessive ROS, we examined gene expressions that involved in oxidative stress and antioxidant defense using a pathway-focused PCR array. We found that expression of antioxidant and ROS metabolism related genes was significantly down-regulated and/or dysregulated in the cochlear tissues of *Cmah*-null mouse. These observations suggested that oxidative stress in the cochlear tissues of *Cmah*-null mouse played an important role in the pathogenesis of AHL.

In this study, we found that Wnt signaling (*Lrp5*, *Lrp6*, *Wnt3a*, *Wnt5a*, *Gsk3 β* , and *Catenin*)- and mitochondrial molecular transport (*Crb1*, *Mtfp1*, *RhoT2*, *Soc2*, and *Atp5f1*)-regulator gene expressions in the cochlear tissues of *Cmah*-null mice with AHL were significantly down-regulated. Previous studies suggest that Wnt/ β -catenin signaling play an important role in critical hepatic development, regeneration, and carcinogenesis [37-39]. The data from these studies suggested that β -catenin regulate hepatic energy metabolism and mitochondrial function [40]. Further, studies from mammalian cells and *Caenorhabditis elegans* showed that β -catenin and Foxos expression in response to oxidative stress have a cross-talk mechanism [41, 42]. Taken our data with previous observations, ROS accumulations in the cochlear tissues of *Cmah*-null mouse might be caused by reduction of both antioxidant- and Wnt/ β -catenin signaling-related gene expressions, which ultimately induced mitochondrial dysfunction (Table 3 and Fig. 4). In conclusion, these findings suggest that *Cmah* disruption could affect a variety of signaling pathways accompanying orchestrated gene expression changes. To the best of our knowledge, our results for the first time showed that down-regulated β -catenin expression in Wnt signaling give rise to ROS in the cochlear tissues of *Cmah*-null mice with AHL (Table 3).

Finally, we found that *Hif1a* and *Foxo3a* mRNAs as well as *Foxo1* and *MnSod* mRNAs expressions, which located in downstream of *Sirt3* gene expression, is significantly decreased. Also, we found that *Sirt3* mRNA expression in the cochlear tissues of *Cmah*-null mouse is significantly down-regulated (Fig. 4). It is well known that *Sirt3* are localized in mitochondria and that *Sirt3* is the primary deacetylase, which plays an important role in energy production, metabolism,

apoptosis, and cell signaling during aging [43-45]. Further, recent several studies also showed that Sirt3 is as an essential player to enhance glutathione antioxidant defense system in mitochondria under CR conditions and demonstrated that Sirt3-dependent mitochondrial adaptations may be a central mechanism of aging retardation in mammals [29, 46, 47]. These observation suggested that ROS accumulations in the cochlear tissues of *Cmah*-null mice with AHL down-regulated Sirt3 expression. As a result, Sirt3 dysregulation leads to oxidative damage and mitochondrial dysfunction (Fig. 4). Therefore, this study could provide a possible mechanism of Sirt3 in ROS and oxidative stress induced metabolism in *Cmah*-null mouse. Based on our results and previous reports, we suggested a hypothetical model that down-regulated Sirt3 lead to oxidative damage and mitochondrial dysfunction and could be alter various signaling pathways in *Cmah*-null mice with AHL. In conclusion, the present study suggests that mice with *Cmah* deficiency serve an important model for studying hearing loss with aging caused by evolutionary loss of Neu5Gc synthesis in human.

Of course, mice studies are not complementary to human. Furthermore, we cannot expect that mice with a human-like deficiency of Neu5Gc will mimic all consequences of Neu5Gc loss in a hominid ancestor. In this study, we selected *Cmah*-null mice as a model system to represents a state of at least partial characterization of biochemistry, physiology and metabolism and it could serve as a model system for studying hearing loss with aging caused by evolutionary loss of Neu5Gc synthesis in human. However many additional studies are required to prove hearing loss with aging caused by evolutionary loss of Neu5Gc synthesis in human.

METHODS

Animal ethics. All animal experiments were approved and performed under the guidelines of the Konkuk University Animal Care and Experimentation Community [IACUC approval number: KU12045]. *Cmah* ^{tm1Ykoz} knockout mice were kindly provided by RIKEN Center for Developmental Biology (CDB, Japan).

Immunohistochemistry (IHC)/ immunofluorescence. For histology, inner ears were harvested after intracardiac perfusion with 4% paraformaldehyde, postfixed overnight, decalcified in 8% EDTA, and embedded in paraffin. Sections were stained with Hematoxylin QS for light microscopy. For IHC, the cochlear tissues were fixed with 4% paraformaldehyde and then embedded on slides. After deparaffination and

rehydration in PBS, sections were blocked in background Sniper solution. After washing, the samples were incubated with specific primary antibodies for Neu5Gc (1:200 dilution; Sialix, San Diego, CA, USA), GFAP, NSE, NF, VIM (prediluted; Leica Biosystems Inc. Buffalo Grove, IL, USA), and Sirt3 (1:200 dilution; Santa Cruz Biotechnology, Inc. Dallas, TX, USA) at 4°C overnight. After the incubation, the samples were washed and incubated with horseradish peroxidase-conjugated secondary antibody. Samples were then stained with ImmPACT™ DAB peroxidase substrate (Vector Laboratories; CA, USA) to visualize the signal. Samples were also stained with Hematoxylin QS to provide background information for reference. The samples were mounted using VECTORSHIELD HardSet mounting medium (Vector Laboratories; CA, USA) and observed using fluorescence microscopy (Olympus; Japan). For immunofluorescence, the samples were incubated with primary antibodies for mitochondrial marker (1:1000 dilution, Abcam, Cambridge, UK) at 4°C overnight. After incubate with Alexa Fluor 488-labeled goat anti-mouse (1:500), the samples were mounted using VECTORSHIELD HardSet mounting medium with DAPI (Vector Laboratories) and observed using fluorescence microscopy (Olympus; Japan).

Apoptotic cell staining. The terminal deoxynucleotidyl transferase-mediated nick end labeling (TUNEL) method was employed for detection of apoptosis using the in situ cell detection kit, tetramethylrhodamine red (TMR, red fluorescence) from Roche Applied Science (Lewes, East Sussex, UK) according to the manufacturer's instructions. For detection of the characteristic chromatin condensation and nuclear fragmentation associated with apoptosis, the samples were mounted using VECTORSHIELD HardSet mounting medium with DAPI (Vector Laboratories) and observed using fluorescence microscopy (Olympus; Japan).

Microarray analysis of gene expression. WT- and *Cmah*-null mice with same age (12 months) and genetic background (C57BL/6J) were used (n=3 per each group) for microarray analysis. Total RNA was extracted and purified from the cochlear tissues of WT- and *Cmah*-null mice using Trizol and RNeasy columns (Qiagen; Valencia, CA, USA) according to the manufacturer's protocol. The RNA quality was verified using an Agilent Bioanalyzer 2100 (Agilent Technologies; Palo Alto, CA, USA) using the RNA 6000 Pico Assay. Generation of double-stranded cDNA, preparation and labeling of cRNA, hybridization to Mouse Ref-8 v2.0 Expression BeadChip (Illumina, Inc.; San Diego, CA, USA), washing, and scanning were all

performed according to the standard Illumina protocol. Arrays were scanned using the Illumina Bead Array Reader Confocal Scanner. Microarray data have been deposited in NCBI's Gene Expression Omnibus and are accessible through GEO Series accession number GSE70659 (Gene expression profile in the cochlear tissue of *Cmah*-null mouse).

In silico data analysis. Differentially expressed genes (DEG) were subjected to intensive investigation to identify their biological functions. GO analysis was performed as described using DAVID (<http://david.abcc.ncifcrf.gov>) to study the biological function of the regulated genes [48]. The differentially expressed genes were compared to all of the genes on the microarrays and a P value computed using a Fisher's exact test. KEGG is a collection of online databases dealing with genomes, enzymatic pathways, and biological chemicals [49]. The KEGG PATHWAY Database records networks of molecular interactions in the cell that includes organism-specific network maps (<http://www.genome.jp/kegg/>). In addition, canonical pathways and functions analyses were created by IPA (Ingenuity Systems, Mountain View, CA, USA), which assists with microarray data interpretation via grouping DEG into known functions, pathways and gene interaction networks, based primarily on human and rodent studies. Significance was set at a P value of 0.05.

Pathway-focused PCR array. The Mouse Oxidative Stress and Antioxidant Defense RT² Profiler™ PCR array (SABiosciences Corp., Valencia, CA) was used to measure the alteration of gene expression in the cochlear tissues from WT- and *Cmah*-null mice. The RT² Profiler™ PCR Array (SABiosciences Corp.) is a commercially available set of optimized RT-qPCR primer assays on a 96-well plate. Total RNA was then treated with DNase I, reverse-transcribed using an RT² First Strand Kit (Qiagen), and brought to a final volume of 120 µL. cDNA from individual samples was used as a template for the PCR array, according to the array instructions, using SYBR green on an ABI ViiA™ 7 system (Applied Biosystems). Data were analyzed using SABiosciences RT² Profiler PCR Data Analysis software, available at <http://pcrdataanalysis.sabiosciences.com/pcr/arrayanalysis.php>, and were considered significant at >4-fold change. Relative quantitation for each gene was determined by normalization to 5 housekeeping genes (*Actb*, *B2m*, *Gapdh*, *Gusb*, and *Hsp90ab1*), comparing the WT and *Cmah*-null groups by using the 2- $\Delta\Delta C_t$ method.

Quantitative real-time polymerase chain reaction (RT-qPCR). The total RNA obtained from the cochlea of WT- and *Cmah*-null mice was reverse-transcribed with

the QuantiTect Reverse Transcription Kit (Qiagen; Valencia, CA, USA) as recommended by the manufacturer. To evaluate gene expression, RT-qPCR was performed on an ABI ViiA™ 7 system (Applied Biosystems; Foster City, CA, USA) with SYBR Green as the fluorescence detection method (Bio-Rad; Hercules, CA, USA). The mouse *Gapdh* gene was used as an internal control to normalize the RT-qPCR efficiency and for quantification of gene expression (Supplementary Table 1 and 2). The RT-qPCR was performed in triplicate for each sample.

Statistical analysis. All experimental data was presented as means \pm standard deviation (SD). Each experiment was performed at least three times. For statistical analysis (Fig. 1 and 4), one-way analysis of variance (ANOVA) was performed to determine whether there were differences among the groups, and Fisher's post-test was performed to determine significance between pairs of groups. In all experiments, *P < 0.05, **P < 0.01, and ***P < 0.001 were considered significant.

ACKNOWLEDGEMENTS

We are thankful to RIKEN Center for Developmental Biology (CDB, Japan) for *Cmah* <tmlYkoz> knockout mice.

Funding

This work was partially supported by Woo Jang-Choon project (PJ007849) from the Rural Development Administration (RDA) and Science Research Center (2015R1A5A1009701) from National Research Foundation of Korea, Republic of Korea.

Conflict of interest statement

The authors declare no conflict of interests.

REFERENCES

1. Muchmore EA, Milewski M, Varki A and Diaz S. Biosynthesis of N-glycolyneuraminic acid. The primary site of hydroxylation of N-acetylneuraminic acid is the cytosolic sugar nucleotide pool. *J Biol Chem.* 1989; 264:20216-20223.
2. Kozutsumi Y, Kawano T, Yamakawa T and Suzuki A. Participation of cytochrome b5 in CMP-N-acetylneuraminic acid hydroxylation in mouse liver cytosol. *J Biochem.* 1990; 108:704-706.
3. Irie A, Koyama S, Kozutsumi Y, Kawasaki T and Suzuki A. The molecular basis for the absence of N-glycolyneuraminic acid in humans. *J Biol Chem.* 1998; 273:15866-15871.
4. Hayakawa T, Satta Y, Gagneux P, Varki A and Takahata N. Alu-mediated inactivation of the human CMP- N-acetylneuraminic acid hydroxylase gene. *Proc Natl Acad Sci U S A.* 2001; 98:11399-11404.

5. Hedlund M, Tangvoranuntakul P, Takematsu H, Long JM, Housley GD, Kozutsumi Y, Suzuki A, Wynshaw-Boris A, Ryan AF, Gallo RL, Varki N and Varki A. N-glycolylneuraminic acid deficiency in mice: implications for human biology and evolution. *Mol Cell Biol.* 2007; 27:4340-4346.
6. Kwon DN, Chang BS and Kim JH. Gene expression and pathway analysis of effects of the CMAH deactivation on mouse lung, kidney and heart. *PLoS One.* 2014; 9:e107559.
7. Kwon DN, Chang BS and Kim JH. MicroRNA dysregulation in liver and pancreas of CMP-Neu5Ac hydroxylase null mice disrupts insulin/PI3K-AKT signaling. *Biomed Res Int.* 2014; 236385.
8. Menardo J, Tang Y, Ladrech S, Lenoir M, Casas F, Michel C, Bourien J, Ruel J, Rebillard G, Maurice T, Puel JL and Wang J. Oxidative stress, inflammation, and autophagic stress as the key mechanisms of premature age-related hearing loss in SAMP8 mouse Cochlea. *Antioxid Redox Signal.* 2012; 16:263-274.
9. Seidman MD, Khan MJ, Bai U, Shirwany N and Quirk WS. Biologic activity of mitochondrial metabolites on aging and age-related hearing loss. *Am J Otol.* 2000; 21:161-167.
10. Yin S, Yu Z, Sockalingam R, Bance M, Sun G and Wang J. The role of mitochondrial DNA large deletion for the development of presbycusis in Fischer 344 rats. *Neurobiol Dis.* 2007; 27:370-377.
11. Tanaka C, Coling DE, Manohar S, Chen GD, Hu BH, Salvi R and Henderson D. Expression pattern of oxidative stress and antioxidant defense-related genes in the aging Fischer 344/NHsd rat cochlea. *Neurobiol Aging.* 2012; 33: e1841-1814.
12. Merksamer PI, Liu Y, He W, Hirschey MD, Chen D and Verdin E. The sirtuins, oxidative stress and aging: an emerging link. *Aging (Albany NY).* 2013; 5:144-150.
13. Jing E, Emanuelli B, Hirschey MD, Boucher J, Lee KY, Lombard D, Verdin EM and Kahn CR. Sirtuin-3 (Sirt3) regulates skeletal muscle metabolism and insulin signaling via altered mitochondrial oxidation and reactive oxygen species production. *Proc Natl Acad Sci U S A.* 2011; 108:14608-14613.
14. Blander G and Guarente L. The Sir2 family of protein deacetylases. *Annu Rev Biochem.* 2004; 73:417-435.
15. Finkel T, Deng CX and Mostoslavsky R. Recent progress in the biology and physiology of sirtuins. *Nature.* 2009; 460:587-591.
16. Donmez G and Guarente L. Aging and disease: connections to sirtuins. *Aging Cell.* 2010; 9:285-290.
17. Finkel T and Holbrook NJ. Oxidants, oxidative stress and the biology of ageing. *Nature.* 2000; 408:239-247.
18. Finley LW, Carracedo A, Lee J, Souza A, Egia A, Zhang J, Teruya-Feldstein J, Moreira PI, Cardoso SM, Clish CB, Pandolfi PP and Haigis MC. SIRT3 opposes reprogramming of cancer cell metabolism through HIF1alpha destabilization. *Cancer Cell.* 2011; 19:416-428.
19. Hirschey MD, Shimazu T, Goetzman E, Jing E, Schwer B, Lombard DB, Grueter CA, Harris C, Biddinger S, Ilkayeva OR, Stevens RD, Li Y, Saha AK, et al. SIRT3 regulates mitochondrial fatty-acid oxidation by reversible enzyme deacetylation. *Nature.* 2010; 464:121-125.
20. Ahn BH, Kim HS, Song S, Lee IH, Liu J, Vassilopoulos A, Deng CX and Finkel T. A role for the mitochondrial deacetylase Sirt3 in regulating energy homeostasis. *Proc Natl Acad Sci U S A.* 2008; 105:14447-14452.
21. Bell EL, Emerling BM, Ricoult SJ and Guarente L. SirT3 suppresses hypoxia inducible factor 1alpha and tumor growth by inhibiting mitochondrial ROS production. *Oncogene.* 2011; 30:2986-2996.
22. Qiu X, Brown K, Hirschey MD, Verdin E and Chen D. Calorie restriction reduces oxidative stress by SIRT3-mediated SOD2 activation. *Cell Metab.* 2010; 12:662-667.
23. Someya S and Prolla TA. Mitochondrial oxidative damage and apoptosis in age-related hearing loss. *Mech Ageing Dev.* 2010; 131:480-486.
24. Sundaresan NR, Gupta M, Kim G, Rajamohan SB, Isbatan A and Gupta MP. Sirt3 blocks the cardiac hypertrophic response by augmenting Foxo3a-dependent antioxidant defense mechanisms in mice. *J Clin Invest.* 2009; 119:2758-2771.
25. Tao R, Coleman MC, Pennington JD, Ozden O, Park SH, Jiang H, Kim HS, Flynn CR, Hill S, Hayes McDonald W, Olivier AK, Spitz DR and Gius D. Sirt3-mediated deacetylation of evolutionarily conserved lysine 122 regulates MnSOD activity in response to stress. *Mol Cell.* 2010; 40:893-904.
26. Hallows WC, Yu W, Smith BC, Devries MK, Ellinger JJ, Someya S, Shortreed MR, Prolla T, Markley JL, Smith LM, Zhao S, Guan KL and Denu JM. Sirt3 promotes the urea cycle and fatty acid oxidation during dietary restriction. *Mol Cell.* 2011; 41:139-149.
27. Perez VI, Van Remmen H, Bokov A, Epstein CJ, Vijg J and Richardson A. The overexpression of major antioxidant enzymes does not extend the lifespan of mice. *Aging Cell.* 2009; 8:73-75.
28. Shi T, Wang F, Stieren E and Tong Q. SIRT3, a mitochondrial sirtuin deacetylase, regulates mitochondrial function and thermogenesis in brown adipocytes. *J Biol Chem.* 2005; 280:13560-13567.
29. Someya S, Yu W, Hallows WC, Xu J, Vann JM, Leeuwenburgh C, Tanokura M, Denu JM and Prolla TA. Sirt3 mediates reduction of oxidative damage and prevention of age-related hearing loss under caloric restriction. *Cell.* 2010; 143:802-812.
30. Chandrasekharan K, Yoon JH, Xu Y, deVries S, Camboni M, Janssen PM, Varki A and Martin PT. A human-specific deletion in mouse Cmah increases disease severity in the mdx model of Duchenne muscular dystrophy. *Sci Transl Med.* 2010; 2:42ra54.
31. Galea E, Launay N, Portero-Otin M, Ruiz M, Pamplona R, Aubourg P, Ferrer I and Pujol A. Oxidative stress underlying axonal degeneration in adrenoleukodystrophy: a paradigm for multifactorial neurodegenerative diseases? *Biochim Biophys Acta.* 2012; 1822:1475-1488.
32. Bao J and Ohlemiller KK. Age-related loss of spiral ganglion neurons. *Hear Res.* 2010; 264:93-97.
33. Jacono AA, Hu B, Kopke RD, Henderson D, Van De Water TR and Steinman HM. Changes in cochlear antioxidant enzyme activity after sound conditioning and noise exposure in the chinchilla. *Hear Res.* 1998; 117:31-38.
34. McFadden SL, Ding D, Reaume AG, Flood DG and Salvi RJ. Age-related cochlear hair cell loss is enhanced in mice lacking copper/zinc superoxide dismutase. *Neurobiol Aging.* 1999; 20:1-8.
35. Fortunato G, Marciano E, Zarrilli F, Mazzaccara C, Intrieri M, Calcagno G, Vitale DF, La Manna P, Saulino C, Marcelli V and Sacchetti L. Paraoxonase and superoxide dismutase gene polymorphisms and noise-induced hearing loss. *Clin Chem.* 2004; 50:2012-2018.
36. Jiang H, Talaska AE, Schacht J and Sha SH. Oxidative imbalance in the aging inner ear. *Neurobiol Aging.* 2007; 28:1605-1612.
37. Thompson MD and Monga SP. WNT/beta-catenin signaling in liver health and disease. *Hepatology.* 2007; 45:1298-1305.
38. Monga SP. Role of Wnt/beta-catenin signaling in liver metabolism and cancer. *Int J Biochem Cell Biol.* 2011; 43:1021-1029.

39. Behari J, Yeh TH, Krauland L, Otruba W, Cieply B, Hauth B, Apte U, Wu T, Evans R and Monga SP. Liver-specific beta-catenin knockout mice exhibit defective bile acid and cholesterol homeostasis and increased susceptibility to diet-induced steatohepatitis. *Am J Pathol.* 2010; 176:744-753.
40. Lehwald N, Tao GZ, Jang KY, Papandreou I, Liu B, Pysz MA, Willmann JK, Knoefel WT, Denko NC and Sylvester KG. beta-Catenin regulates hepatic mitochondrial function and energy balance in mice. *Gastroenterology.* 2012; 143:754-764.
41. Essers MA, de Vries-Smits LM, Barker N, Polderman PE, Burgering BM and Korswagen HC. Functional interaction between beta-catenin and FOXO in oxidative stress signaling. *Science.* 2005; 308:1181-1184.
42. Hoogeboom D, Essers MA, Polderman PE, Voets E, Smits LM and Burgering BM. Interaction of FOXO with beta-catenin inhibits beta-catenin/T cell factor activity. *J Biol Chem.* 2008; 283:9224-9230.
43. Kong X, Wang R, Xue Y, Liu X, Zhang H, Chen Y, Fang F and Chang Y. Sirtuin 3, a new target of PGC-1alpha, plays an important role in the suppression of ROS and mitochondrial biogenesis. *PLoS One.* 2010; 5:e11707.
44. Buler M, Aatsinki SM, Izzi V and Hakkola J. Metformin reduces hepatic expression of SIRT3, the mitochondrial deacetylase controlling energy metabolism. *PLoS One.* 2012; 7:e49863.
45. D'Aquila P, Rose G, Panno ML, Passarino G and Bellizzi D. SIRT3 gene expression: a link between inherited mitochondrial DNA variants and oxidative stress. *Gene.* 2012; 497:323-329.
46. Haigis MC and Guarente LP. Mammalian sirtuins--emerging roles in physiology, aging, and calorie restriction. *Genes Dev.* 2006; 20:2913-2921.
47. Han C and Someya S. Maintaining good hearing: calorie restriction, Sirt3, and glutathione. *Exp Gerontol.* 2013; 48:1091-1095.
48. Huang da W, Sherman BT and Lempicki RA. Systematic and integrative analysis of large gene lists using DAVID bioinformatics resources. *Nat Protoc.* 2009; 4:44-57.
49. Kanehisa M and Goto S. KEGG: kyoto encyclopedia of genes and genomes. *Nucleic Acids Res.* 2000; 28:27-30.